Long-range hydrodynamic correlations in quasi-one-dimensional circular and straight geometries

Ekaterina Kosheleva, Brian Leahy, Haim Diamant, Binhua Lin, and Stuart A. Rice

Phys. Rev. E **86**, 041402 — Published 31 October 2012

DOI: 10.1103/PhysRevE.86.041402

Long Range Hydrodynamic Correlations in Quasi-One-Dimensional Circular and Straight Geometries

Ekaterina Kosheleva[1], Brian Leahy[2], Haim Diamant[3], Binhua Lin[4,*] & Stuart A. Rice[5,*]

[1]*Department of Physics, Harvard University, Cambridge, Massachusetts 02138, USA*

[2]*Department of Physics, Cornell University, Ithaca, New York, 14850, USA*

[3]*Raymond & Beverly Sackler School of Chemistry, Tel Aviv University, Tel Aviv 69978, Israel*

[4]*The James Franck Institute & CARS, The University of Chicago, Chicago, Illinois 60637, USA*

[5]*Department of Chemistry & The James Franck Institute, The University of Chicago, Chicago, Illinois 60637, USA*

We report the results of studies of the collective and pair diffusion coefficients of particles in two quasi-one-dimensional geometries: straight 2 mm long channels and rings with radii between 3 and 35 μm. We find a contribution to the packing fraction dependence of the collective diffusion coefficient that confirms the behavior predicted by Frydel and Diamant (Phys. Rev. Lett. **104**, 248302 (2010)), indicative of long-range hydrodynamic coupling resulting from collective motion of particles in periodic quasi-one-dimensional geometries. Specifically, we find a proportionality constant of 0.19 ± 0.01 $\mu m^2/s$ between the residual collective diffusion coefficient (defined as the collective diffusion coefficient less the mean self diffusion coefficient of colloids) and the packing fraction for the ring geometries, independent of ring curvature, and a proportionality constant of 0.14 ± 0.01 $\mu m^2/s$ for 2 mm straight channels. Both of these values, for circular geometries in particular, are significantly larger than predicted when only ensemble averaging over particle positions is accounted for, which strongly suggests the presence of additional hydrodynamic coupling. These findings are signficant because they imply that the global geometry of the confined suspension influences collective colloidal diffusion even when single file motion of colloids is maintained.

*Corresponding authors: Binhua Lin (lin@cars.uchicago.edu) and Stuart A. Rice (s-rice@uchicago.edu)

I. Introduction

Colloids constrained to diffuse in lower dimensional systems have been observed to interact hydrodynamically in ways that are vastly different with regards to diffusion in an unbounded system. These systems, aside from being ubiquitous in nature (appearing, for example, in the transport of materials across porous media and the transport of blood through arteries [1, 2]), exhibit hydrodynamic interactions that are interesting in their own right. In particular, the strict confinement of a suspension changes the spatial decay of the hydrodynamic interactions between particles, the concentration dependence of these interactions, and even their sign [3, 4]. To date, great strides have been made in understanding these hydrodynamic effects. In particular, the long-range form of the pair interaction has been investigated experimentally and theoretically in quasi-one-dimensional (q1D)[4-7], and quasi-two-dimensional (q2D) [3, 4, 8] systems, and also in the crossover regime between q1D and q2D [9] and between q2D and 3D [10] confinement. Yet there remain other hydrodynamically influenced properties of q1D and q2D suspensions that have not been adequately explained.

Digital video microscopy is used in our studies of collective diffusion in the "small q" regime of the Fourier space decomposition of the fluid density, encompassing many-body and collective particle motion. Such an experimental system is well suited for studying contributions to collective mobility that are negligible on the scale of short-range interactions. In particular, whereas the boundary conditions at the ends of q1D channels affect the mobility of a single particle only negligibly, recent theoretical work suggests that they have a significant influence on the collective mobility. Specifically, it has been predicted that in a hard-rod fluid constrained to have a periodic q1D geometry, as in a ring or a channel open at both ends to baths of fixed pressure, there will be a hydrodynamic contribution to the collective mobility at density wave-vector $q = 0$ [11]. In this mode, the system diffuses collectively, with particles displacing the entire liquid column between

them as they diffuse. In geometries where this effect is present, the corresponding contribution to the collective diffusion coefficient is predicted to scale with the q1D packing fraction $\eta = \sigma N/L$, where σ is the particle diameter, and N/L is the average number of particles in the channel per unit length. Thus, the collective motion of q1D particles is determined by both the presence of hard confining walls, which force the single file diffusion of the colloids, and by the end boundary conditions influencing the confinement of the fluid suspension.

In this paper we report the results of an explicit test of the predicted influence of the longitudinal hydrodynamic modes on collective diffusion in q1D suspensions. Although a correlation between the collective diffusion coefficient and the colloid packing fraction has previously been observed in q1D suspensions by Xu et al [7], in this paper we seek to rigorously examine this correlation, both measuring its functional form and offering the first explanation as to its cause. In addition, we report a study of how narrow channel geometries affect the collective diffusion of colloids confined to single file motion via examination of particle motion over a large range of colloid packing fractions in rings with radii between 3 μm and 35 μm and in 2 mm straight channels. The observed packing fraction dependence of the collective diffusion coefficient in rings, relative to that in straight channels, confirms the prediction of Ref. [11] concerning the $q = 0$ hydrodynamic contribution to the packing fraction dependence of collective particle motion in a ring.

We emphasize to the reader that the system studied in this paper differs fundamentally from that studied by Sokolov et al [12]. In our system the particles are confined in a circular channel by walls, and the focus of attention is on the contribution to diffusive motion of longitudinal modes in the infinite wavelength limit. The diffusive motion is studied in the quiescent colloid suspension. The presence of the walls defines, via the boundary conditions at the walls, the character of the hydrodynamics. In the system studied by Sokolov et al, the particles are driven by an external force in a circular path in an unbounded fluid. Consequently, the hydrodynamic interaction between

particles propagates in all directions and is not altered by boundary conditions at the walls of a confining channel. The focus of attention in the work of Sokolov et al is on the effective non-equilibrium attraction between a pair of particles generated by the symmetry breaking of the driven motion of a particle on the closed circular path.

II. Background and Theory

Previous hydrodynamic analyses of q1D colloid suspensions have discounted the presence of longitudinal modes in the host liquid, modeling the system as an incompressible fluid in a sealed channel of finite length. These assumptions are based on the physical argument that a 1D mass dipole (the model for a 1D source of longitudinal flow) creates a uniform flow response along the channel length, which under no-slip boundary conditions at the channel edges effectively determines that the induced flow (integrated over the cross-section of the channel) vanishes along the entire channel length.

Thus, only considering transverse flow, the Stokeslet approximation (portraying the source particle as a unit point force in the fluid) yields an Oseen tensor that decays exponentially at distances $x >> \sigma/H$, for particle diameter σ and channel width H [4]. This exponential decay has been verified from measurements of the pair diffusion coefficient, even in regimes where $x >> \sigma/H$ is not strictly appropriate [6]. Under the necessary assumptions for the Stokeslet approximation to hold, namely that $\sigma << x$, and $\sigma << H$, and also assuming that the colloid diffuses along the axis of a cylindrical channel of radius H, the pair mobility is given by the Green's function solution of the Stokes equation for this geometry [6]:

$$G_{xx}(x) = (8\pi\mu H)^{-1} \times$$

$$\begin{cases} [a_1 \cos(\beta_1 x/H) + b_1 \sin(\beta_1 x/H)]e^{-\alpha_1 x/H} & x >> H \\ 2H/x & x << H \end{cases} \qquad (1)$$

where μ is the fluid shear viscosity, and $a_1 \approx -0.0370, b_1 \approx 13.8, \alpha_1 \approx 4.47, \beta_1 \approx 1.47$. Corrections to this solution to account for the non-zero size of the particle and reflections of fluid from the channel walls, calculated using the method of reflections, have been reported by Xu et al [7].

The situation is complicated when the no-slip boundary condition at the channel ends no longer holds, a condition that is associated with many if not most q1D systems. Such systems include not only the toy theoretical model of an infinite length channel, but also channels exhibiting periodic boundary conditions, and finite channels with open ends, i.e., ends which allow fluid to flow in and out freely. In these geometries, the boundary conditions no longer dictate that longitudinal modes must vanish. Hydrodynamic behavior in such geometries has been studied theoretically using a simplified phenomelogical approach that only retains longitudinal components of the liquid flow. In this approach, particles and channels are once again assumed rigid with no-slip boundaries but, in addition, interaction with boundaries is averaged and approximated by an effective friction term α, which greatly simplifies many aspects of the calculation. Under these assumptions the linearized 1D hydrodynamic equations are given by

$$\rho_0 \dot{u} = -p' + (4\mu/3 + \zeta)u'' - (\alpha\mu/H^2)u + (\beta/H^2)f$$
$$\dot{\rho} = -\rho_0 u', \quad p = c_s^2 \rho \tag{2}$$

in which a dot denotes a time-derivative, a prime a spatial derivative, and *ρ(x,t), p(x,t)* and *u(x,t)* are displacements in liquid density, pressure and velocity about ρ_0, p_0 and 0, respectively, in response to a force density (per unit length) of $f(x,t)$. Here, μ and ζ are the shear and bulk viscosity of the ambient fluid, respectively, β is the ratio between H^2 and the cross-sectional channel area, and c_s is the velocity of sound in the fluid. Solving for the hydrodynamic flow, in this case, amounts to solving for the velocity Green's function $G(x,t) = u(x,t)$ for an applied point force $f(x,t) = \delta(x)\delta(t)$.

This problem has been solved explicitly in Ref. [11]. In particular, it has been found that at steady state ($\omega = 0$ for the Fourier inverted time coordinate ω), $G(q \neq 0, \omega = 0) = 0$, implying that longitudinal modes vanish on length scales smaller than the total length of the colloidal system. However,

$$G(q = 0, \omega = 0) = \frac{\beta}{\alpha \mu} \tag{3}$$

which implies a long-range hydrodynamic correlation at steady state, which can be understood intuitively as originating from collective motion of particles in one direction in a hard-rod fluid.

It is shown in Ref. [11] that this hydrodynamic correlation has a non-trivial effect in the regime of collective diffusion of the particles, which we will now relate to the quantities measured in our experiments. According to the fluctuation-dissipation theorem (remembering that the Green's function solution of the Stokes equation is equivalent to the large-distance particle pair mobility (in the limit of very small particles),

$$D_{12} = \gamma \, k_B T \, G(x, \omega = 0) \tag{4}$$

where

$$D_{12} = \langle \Delta x_1(t) \Delta x_2(t) \rangle / 2t \tag{5}$$

is the residual pair diffusion coefficient between particles 1 and 2, T the fluid temperature, $\Delta x_i(t)$ the displacement of particle i at time t, and γ a constant dependent on the ratio σ/H, tending to unity as $\sigma/H \to 0$.

The contribution of flow correlations between particles to the collective diffusion can be obtained by summing D_{12} over all particle pairs. The collective diffusion coefficient is defined as

$$D_{col} = N \cdot D_{cm} = \langle (\sum_{i=0}^{N} \Delta x_i)^2 \rangle / 2\ N\ t \tag{6}$$

where N is the number of particles in the system and D_{cm} is the diffusion coefficient of the center of mass. The portion of D_{col} accounting for flow correlations between particles, dubbed the *residual* collective diffusion $\overline{D_{col}}$, is given by

$$\overline{D_{col}} = D_{col} - D_s \tag{7}$$

$$D_s = \frac{\langle (\Delta x)^2 \rangle}{2t} \tag{8}$$

where D_s is the one-particle self-diffusion coefficient. This definition takes the contribution from flow correlations to be given by the difference between the collective and self diffusion coefficients, taking advantage of the fact that the former measures colloid diffusion including the effects of flow correlations between particles, and the latter measures contributions to colloid diffusion without them. Thus,

$$\overline{D_{col}} \equiv D_{col} - D_s = \frac{1}{N} \sum_{i,j=1, i \neq j}^{N} D_{12}(r_{ij}) \tag{9}$$

where r_{ij} is the radial distance between particles *i* and *j*. The value of $\overline{D_{col}}$ resulting *only* from the predicted contribution at $q=0$, dubbed $\overline{D_{col,long}}$, can be computed explicitly for the case of an

infinite channel (or, equivalently a channel with periodic boundary conditions) such that the particles are regularly spaced a distance d. In this case, using Eqs. (3), (4) and (9), we obtain

$$\overline{D_{col,long}}/(\gamma k_B T) = [2\sum_{n=1}^{\infty} G(x = nd, \omega]_{\omega \to 0} = \beta/\alpha\mu d \, .$$

If the particles are Brownian and randomly sample all separations d, we should replace the $1/d$ factor by its average, which is the mean linear density, $N/L = \eta/\sigma$. Thus,

$$\overline{D_{col,long}}/(\gamma k_B T) = (\beta/\alpha\mu\,\sigma)\,\eta \qquad (10)$$

Additionally, for a system of Brownian particles in thermal equilibrium, all transport coefficients should be dependent on packing fraction because of the ensemble averaging over particle configurations. At low packing fraction that dependence should be linear. For the collective diffusion coefficient, using Eq. (9), we have,

$$\left\langle \overline{D_{\rm col}} \right\rangle = \frac{1}{N} \sum_{i,j=1, i\neq j}^{N} \left\langle D_{12}(x_{ij}) \right\rangle ; \; 2\sum_{n=1}^{\infty} \left\langle D_{12}(x_n) \right\rangle = 2\sum_{n=1}^{\infty} \int dx_n P_n(x_n) D_{12}(x_n) \, , \qquad (11)$$

where $x_n = |\, x_{ij}|$ is the distance between particles i and j along the channel, $n = |i - j|$, and $\langle \ldots \rangle$ denotes an ensemble average. The second equality in Eq. (11) assumes that the suspension is homogeneous and that the pair hydrodynamic interaction in the channel is short-ranged, i.e., $D_{12}(x)$ decays exponentially with x. The $P_n(x_n)$ are the probability density functions for having two particles separated by a distance x_n with $(n - 1)$ particles in between. Assuming a 1D suspension of hard rods (Tonks gas), we have

$$P_n(x_n) = \frac{1}{n!}\left(\frac{\eta}{\sigma}\right)^n (x_n - n\sigma)^{n-1} e^{-\eta(x_n - n\sigma)/\sigma}, \quad n\sigma < x_n < \infty, \qquad (12)$$

where $\eta = \sigma/d$ is the system packing fraction. Given the pair hydrodynamic interaction in the channel, via $D_{12}(x)$, including its η dependence, Eqs. (11) and (12) allow for the calculation of the full η dependence of $\left\langle \overline{D_{\rm col}} \right\rangle$. We restrict the current discussion, however, to the leading linear

dependence on η, to which only the $n = 1$ (nearest neighbors) term in Eq. (11) contributes. In addition, we empricially fit the pair hydrodynamic interaction to a single exponential function (see Section IV),

$$D_{12}(x) = Ae^{-Bx}. \tag{13}$$

These approximations yield

$$\left\langle \overline{D_{col}} \right\rangle = \frac{2A^{-B\sigma}\eta}{B\sigma}. \tag{14}$$

We now make the key observation that in closed-end channels the thermal averaging of the short-range pair hydrodynamic interactions, which leads to Eq. (14), is the sole origin of the η dependence of $\overline{D_{\mathrm{col}}}$. In circular channels, by contrast, an additional contribution from the long-range, $q = 0$, correlation should be present. To summarize, the measured reduced collective diffusion coefficient should be

$$\overline{D_{\mathrm{col}}} = \left\langle \overline{D_{\mathrm{col}}} \right\rangle + \overline{D_{\mathrm{col,long}}}, \tag{15}$$

where $\overline{D_{\mathrm{col,long}}}$ is the $q = 0$ long-ranged contribution present only in the circular channels given in Eq. (10). Calculations reported in Ref. 11 show, by comparison with lattice Boltzmann simulation results, that the decay of $\overline{D_{\mathrm{col}}}$ with interparticle separation is much slower than expected from the hydrodynamic screening description. In addition to this slower than expected decay of $\overline{D_{\mathrm{col}}}$, the theoretical prediction arising from the current analysis is that for closed-end channels $\overline{D_{\mathrm{col}}}$ should follow Eq. (14), whereas for the circular channels a larger proportionality coefficient between $\overline{D_{\mathrm{col}}}$ and η should be found. Thus, observation of an increase in the coefficient describing η dependence of $\overline{D_{\mathrm{col}}}$ will be a signature, albeit indirect, of the existence of long-ranged hydrodynamic correlations in the circular channels.

III. Experimental Details

Our experimental system consists of an aqueous solution of silica particles (1.57 ± 0.04 μm, mass density 2.2 gm/cm^3, Duke Scientific), confined to move in circular or straight one-dimensional channels (3 μm × 3 μm cross section) printed on a polydimethylsiloxane (PDMS) mold and bounded above by a glass coverslip. The straight channels used in the experiment were 2 mm in length, and the 8 different ring radii ranged from 3 to 35 μm. Different radii offer the benefit of testing for a possible curvature dependence of the collective, correlated motions of the particles, and ease the collection of data over a large range of η.

To start the experiment, an aqueous solution of silica particles is prepared (~0.5 μL -2 $\underline{\mu L}$ spheres per 1 mL water). About 30 μL of this solution is placed over a pattern of circular or straight channels, between two PDMS spacers about 70 μm thick, and then covered by a glass coverslip, leaving a layer of fluid on the order of tens of microns thick between coverslip and mold. Figure 1 shows an image of one particular data set at four different radii and η, and Figure 2 shows a schematic of the experimental setup, reminding the reader of the particular open- top geometry used in the experiments.

Digital video microscopy is then used to track the diffusion of spheres in the channel and extract their time-dependent x- and y-trajectories at time intervals of 0.033 s and 0.005 s. The particles are imaged using an Olympus BH2 metallurgical microscope, a 50x oil-immersion objective (0.80 NA), and a 2.5x video eyepiece. Data were collected for durations between 10 minutes and 2 hours for each η studied.

The particle trajectories were determined using image analysis routines in IDL developed by Crocker and Grier [13], with a spatial resolution of about 20 nm. A more detailed description of the fabrication process for the PDMS mold and data analysis routines is given in our previous papers [5]. The colloid particles in our systems exhibit q1D behavior; namely, the channel is narrow enough that the spheres cannot pass each other, fixing the ordering of the spheres in the channel, and

restricting their motions to the x (or $r \cdot \theta$) direction. In such a setup, particles diffuse as a result of quasi-one-dimensional Brownian motion, due to random thermal interactions with molecules in the supporting fluid and flow correlations generated by nearby particles.

As noted above, the channels that confine the colloid suspensions are unconfined at the top. Nevertheless, the microscope images show that the colloid particle centers lie in the focal plane and remain there for the duration of the experiments. The particles are confined to the channel with a gravitational well potential of about 14 $k_B T$, so particles only rarely jump out of a channel. Furthermore, as shown in earlier studies of colloid suspensions in q1D channels that are unconfined at the top, the influence of hydrodynamic interactions is well accounted for when the channel is represented as a fully closed capillary with effective radius very close to the channel width (and depth). This approximation works because the fluid in the q1D channel and above is quiescent; thus, there must be a boundary in the fluid that contacts the lips of the channel and on which the fluid velocity vanishes. We expect that the same situation exists for the ring channels.

To measure the so-called short-time diffusion coefficient, the mean squared displacements of the particles were measured over 200 ms. This time scale is long compared to the momentum relaxation time of a colloid particle and the establishment of hydrodynamic interactions, but short enough that direct particle-particle interactions do not influence the measured diffusion coefficients.

IV. Results

Our experiments have the goal of resolving three questions pertaining to the collective dynamics of colloid suspensions constrained to occupy various q1D geometries. First, does the longitudinal hydrodynamic correlation in periodic geometries as described by Eq. (10) exist? Second, is there a curvature dependence to the measured pair and collective diffusion coefficients? Third, what can we learn from comparing diffusion in the $q = 0$ and large q regimes, with the latter

obtained from the distance dependence of the pair diffusion coefficients?

IVA. Correlation in Rings

Self and collective diffusion coefficients were determined from the short time-evolution of individual and center of mass mean-squared displacements. Data were collected for suspensions in rings with radii between 3 μm and 35 μm (listed in the description of Figure 1), at packing fractions between 0.04 and 0.8. Figure 3c shows the measured residual collective diffusion coefficients of particles in the circular channels as a function of packing fraction η, while Figures 3a-b display the corresponding self and collective diffusion coefficients at each measured packing fraction. As predicted, $\overline{D_{col}}$ is a linear function of the packing fraction η of particles suspended in the channel. It is especially noteworthy that, while the rate of diffusion of individual particles decreases with increasing η, the mean squared displacement of the entire system nonetheless increases, due in part to the propagation of the longitudinal mode.

It is natural to ask if the ring curvature affects the colloid collective diffusion coefficient. To address this question we also show in Fig. 3c the η dependences of the residual collective diffusion coefficients for different ring radii. To the resolution of our experiment, for circular channels with radii between 3 μm and 35 μm there does not appear to be a measurable curvature dependence of the collective diffusion coefficient of the system.

IVB. Correlation in Straight Channels

Self and collective diffusion coefficients were determined from the short time-evolution of individual and center of mass mean-squared displacements for suspensions in straight channels at η comparable to those used for suspensions in ring channels. These diffusion coefficients can be characterized as N-particle cluster diffusion coefficients with a large N. It has previously been

observed by Xu et al [14] that the *N*-particle cluster diffusion coefficient approaches the collective diffusion coefficient for sufficiently large *N*, and in the cases considered in this paper *N* is sufficiently large that the inferred collective diffusion coefficient differs negligibly from that of an infinite system. Figure 4c displays the residual collective diffusion coefficient as a function of packing fraction, while Figures 4a-b display the corresponding self and collective diffusion coefficients at each measured packing fraction. Clearly, just as in the case of colloid suspensions in circular channels, the collective diffusion coefficient is a linear function of the system packing fraction. However, Figure 5, which overlays the residual collective diffusion coefficients measured in the two data sets, displays a clear difference between the magnitudes of the η dependences of $\overline{D_{\mathrm{col}}}$ for the two confining geometries. Fitting the measured pair diffusion coefficient (see Section IV.C) to Eq. (13), we find $A = 0.18 \pm 0.01$ μm^2/s and $B = 0.71 \pm 0.02$ μm^{-1}. Substituing these values in Eq. (14), we predict $\langle\overline{D_{col}}\rangle/\eta = 0.11 \pm 0.01$ μm^2/s (Fig. 5). This fit, although somewhat smaller than the measured η dependence for the straight channels, accounts for almost all of the linear dependency in the straight channels, but cannot account for the slope of η dependence in the ring systems, suggesting that the longitudinal mode is a non-negligible contributor to collective diffusion in these geometries.

IV.C Colloid Pair Diffusion in Circular and Straight Channels

Finally, we examine the pair-correlation coefficients, $D_{12}(x)$, of both geometries in the large *q* regime, in light of the behavior of the collective diffusion in the small *q* regime, using, as vehicle, the normalized pair-diffusion coefficient Δ :

$$\Delta = HD_{12}(x)/(aD_0) \tag{16}$$

where a is the particle radius, x the separation between the two particles, D_0 the unbounded self-diffusion coefficient and H the cross-sectional width of the channel. The parameter Δ has previously been measured for straight channels [6], and its x dependence found to be dominated by transverse modes, exhibiting an exponential decay as a function of x. From our data set we obtain Δ for a variety of different curvatures and η, which are shown in Figure 6. Note that in Figs 6-8 the pair diffusion coefficients of lower η samples were derived by sampling all possible particle pairs in the channel, whereas that of higher η samples were derived by sampling pairs that are nearest neighbors in order to remove the oscillilation of the curve due to the effect of the pair-distribution function [7].

First, we use these data to determine the accuracy of the empirical Eq. (13). Figure 7 displays Δ derived from combining data from circular channels with lower and higher colloid η (the cutoff between the two categories being roughly $\eta = 0.45$), which greatly improves the statistics of the data and resulting fit. Fig. 7 also displays an exponentially decaying fit of Δ from the data at lower η, which contains the better statistics of the two data sets. Rescaling the fit values in Fig. 7 from Δ in Eq. (16) back to D_{12} in Eq. (13) we find $A = 0.18 \pm 0.01$ μm^2/s and $B = 0.71 \pm 0.02$ μm^{-1}.

Finally, Figure 8 overlays previously measured (η independent) pair diffusion coefficients for straight q1D channels with measured pair diffusion coefficients at various η for the rings with different curvatures. To the resolution of our measurements, there is no measurable difference between pair diffusion coefficients in these two constrained geometries, supporting the hypothesis that end boundary conditions do not significantly affect particle correlations in the high q regime. Furthermore, in all of our data we find no measurable dependence of the pair diffusion coefficients on ring curvature (Fig. 6) or colloid η (Figs. 6-8).

V. Discussion

Our experiments demonstrate the influence of the longitudinal hydrodynamic mode

predicted in Ref. [11] on colloid diffusion in a circular channel. As theoretically predicted, we have found a larger proportionality coefficient between the residual collective diffusion coefficient and packing fraction in the circular channels (Fig. 5) compared to that of the straight channels. This increase in η dependence is an indication of the long-range hydrodynamic correlations present in the circular systems, which obey periodic boundary conditions, as opposed to the closed-end channels.

The evidence, however, is indirect. One may raise other aspects, in which the two types of channels differ, and which might be responsible for the different η dependencies. (i) The channel geometry (straight vs. curved) might affect the collective diffusion. Yet, if curvature mattered, we would see differences between rings with different radii, with the results for the larger rings tending toward those of the straight channel. No such trend is seen in Fig. 3c. (ii) The finite length of the channel might also play a role in the measured collective diffusion. Here, again, if that were a significant effect, we would see it in the results for different ring sizes. To these geometrical arguments we add the following observations. (iii) The dependence of the self-diffusion coefficient on particle packing fraction is the same, within experimental error, for the various channels (Figs. 3a and 4a). (iv) Nor does the pair diffusion coefficient show sensitivity to the type of channel or its curvature (Fig. 6, Fig. 8). These last two observations imply that the type of channel (straight or curved; close-ended or circular) has no appreciable effect on the *short-ranged* hydrodynamic interactions. Therefore, we argue that the evidence for the role of long-range flows in the collective diffusion of particles in the circular channels, though indirect, is quite compelling. Thus, while Figs. 6-8 demonstrate that particle diffusion is dominated by transverse hydrodynamic modes in the large q regime, the nonvanishing longitudinal mode at $q=0$ nonetheless emerges as a significant contributor to hydrodynamic interactions on the scale of collective, system-wide diffusion.

V. Acknowledgements

This work was supported by the NSF MRSEC (DMR-0820054) at the University of Chicago. HD acknowledges the support from the Israel Science Foundation (Grant No. 8/10). BL acknowledges the support from ChemMatCARS (NSF/CHE-0822838) at the University of Chicago.

References

[1] D. J. Aidley, and P. R. Stanfield, *Ion Channels: Molecules in Action* (Cambridge University Press, New York, 1996).
[2] J. Karger, and D. M. Ruthven, *Diffusion in Zeolites and Other Microporous Solids* (Wiley, New York, 1992).
[3] B. Cui, H. Diamant, B. Lin, and S. A. Rice, Physical Review Letters **92**, 258301 (2004).
[4] H. Diamant, Journal of the Physical Society of Japan **78**, 041002 (2009).
[5] B. Cui, B. Lin, S. Sharma, and S. A. Rice, Journal of Chemical Physics **116**, 3119 (2002).
[6] B. Cui, H. Diamant, and B. Lin, Physical Review Letters **89**, 188301 (2002).
[7] X. Xu, S. A. Rice, B. Lin, and H. Diamant, Physical Review Letters **95**, 158301 (2005).
[8] S. A. Rice, B. Lin, B. Cui, and H. Diamant, Journal of Physics: Condensed Matter **17**, 1 (2005).
[9] S. Novikov, S. A. Rice, B. Cui, H. Diamant, and B. Lin, Physical Review E **82**, 031403 (2010).
[10] V. Prasad, and E. R. Weeks, Physical Review Letters **102**, 178302 (2009).
[11] D. Frydel, and H. Diamant, Physical Review Letters **104**, 248302 (2010).
[12] Y. Sokolov, D. Frydel, D. G. Grier, H. Diamant, and Y. Roichman, Physical Review Letters **107** (2011).
[13] J. C. Crocker, and D. G. Grier, Journal of Colloid and Interface Science **197**, 298 (1996).
[14] X. Xu, B. Lin, B. Cui, A. R. Dinner, and S. A. Rice, Journal of Chemical Physics **132** (2010).

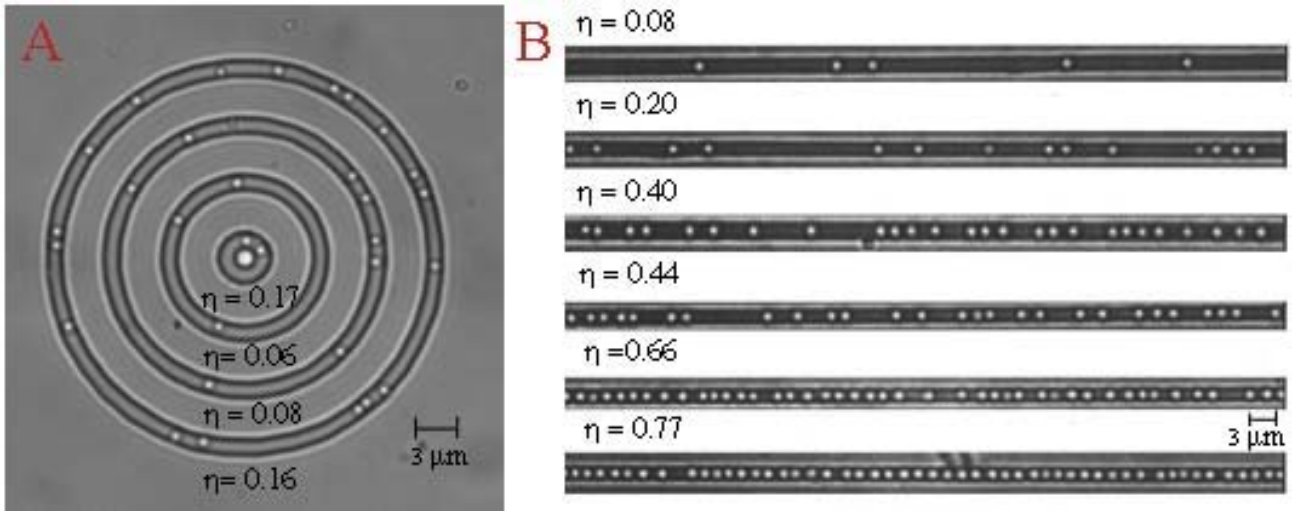

Figure 1: Images of the two mold geometries used in this experiment. (A) The PDMS mold with rings of 4 different radii: 3, 13, 23, and 30 μm, along with the q1D packing fraction η of particles in each channel. Additional ring mold patterns with radii 8, 17, 26, and 35 μm were also used in the experiments. (B) The 2 mm straight channel mold geometries used, along with the q1D packing fraction η of particles in each channel (the field of view shown is 106 μm).

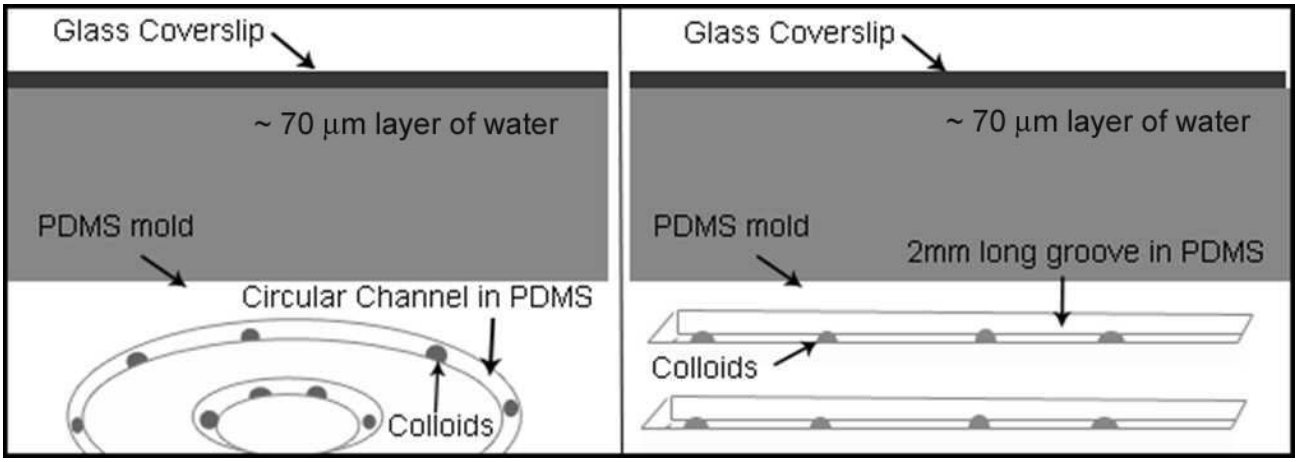

Figure 2: Schematic of the particular open-top geometry used in the experiments, for ring and straight channels.

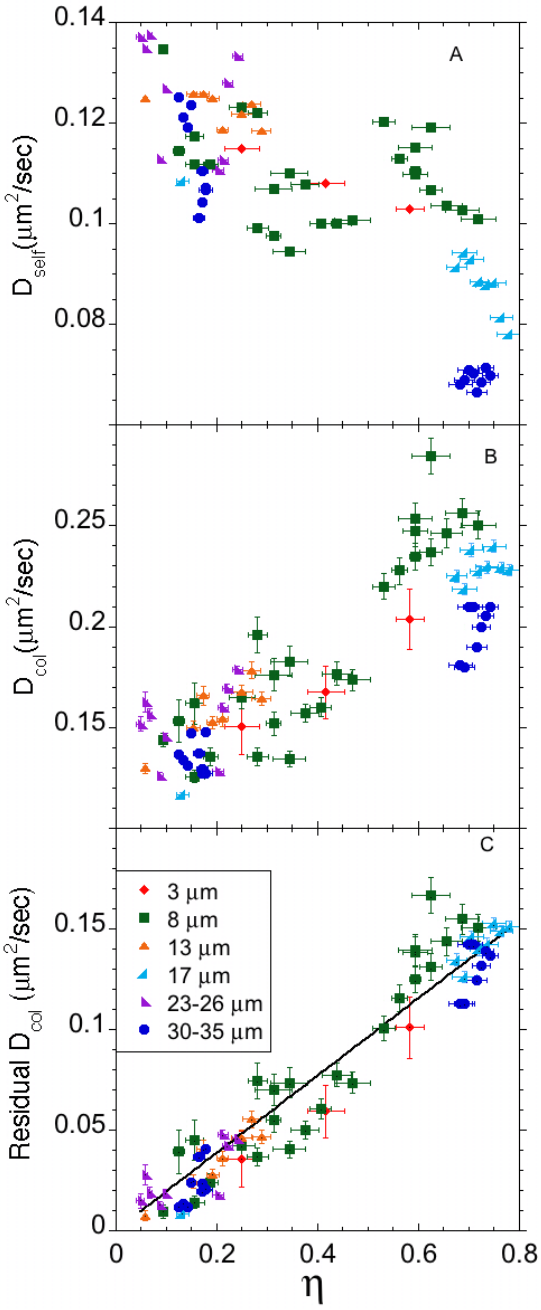

Figure 3: Color online. Self diffusion coefficient $\boldsymbol{D_{self}}$ (A), collective diffusion coefficient $\boldsymbol{D_{col}}$ (B), and residual collective diffusion coefficient $\overline{\boldsymbol{D_{col}}}$ (C) vs. q1D packing fraction for particles in circular channels. The predicted linear η dependence is clearly present in plot (C), in which the linear fit of $\overline{\boldsymbol{D_{col}}}$ v.s. η, $\overline{\boldsymbol{D_{col}}} = (0.19 \pm 0.01)\eta$ $\mu m^2/s$, is plotted. Thermal averaging and the predicted contribution from system-wide collective motion both contribute to the measured slope. Note that there is no apparent curvature dependence to any of the measured values.

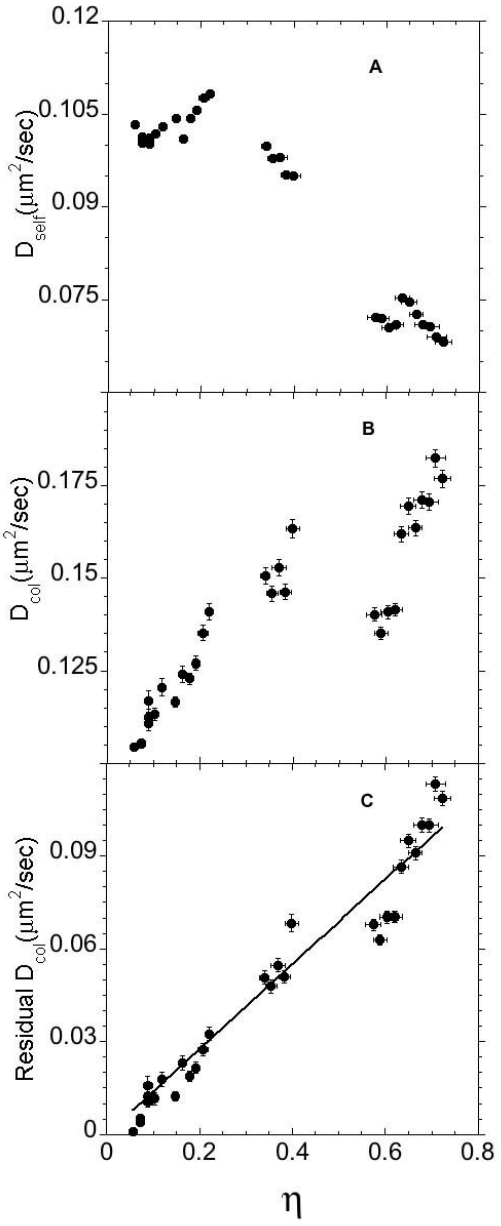

Figure 4: Self diffusion coefficient $\boldsymbol{D_{self}}$ (A), Collective diffusion coefficient $\boldsymbol{D_{col}}$ (B), and residual collective diffusion coeffient $\overline{\boldsymbol{D_{col}}}$ (C) vs. η for particles in straight channels. The predicted linear dependence of $\overline{\boldsymbol{D_{col}}}$ is present in plot (C) (the solid line in 4.C is the result of the linear fit $\overline{\boldsymbol{D_{col}}} = (0.14 \pm 0.01)\eta$ μm²/s), but it is noteworthy that the strength of the linear dependence is markedly smaller than the one in Fig. 3 (C), most likely due to the absence of the collective mode in this geometry.

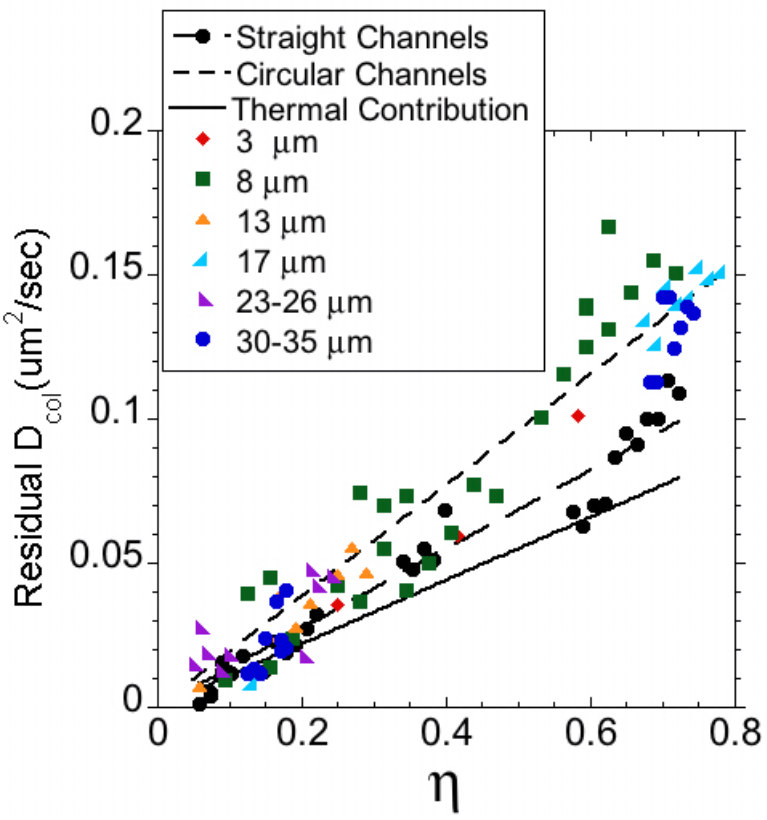

Figure 5: Color online. $\overline{\boldsymbol{D_{col}}}$ for straight and circular geometries, along with the theoretical prediction for the contribution to collective diffusion arising *solely* from thermal fluctuations. The line with short dashes is the linear fit to the data from the circular channels, $\overline{\boldsymbol{D_{col}}} = (0.19 \pm 0.01)\eta$ µm^2/s; the line with long dashes is the fit to the data from the straight channels, $\overline{\boldsymbol{D_{col}}} = (0.14 \pm 0.01)\eta$ µm^2/s; and the solid line is the theoretical prediction not including the longitudinal mode (see text), $\overline{\boldsymbol{D_{col}}} = (0.11 \pm 0.01)\eta$ µm^2/s. The linear dependence for straight channels is dominated by the thermal contribution, whereas the collective diffusion in the ring geometries has a significant larger density dependence, which we claim arises from the collective motion mode at density wavevector q=0.

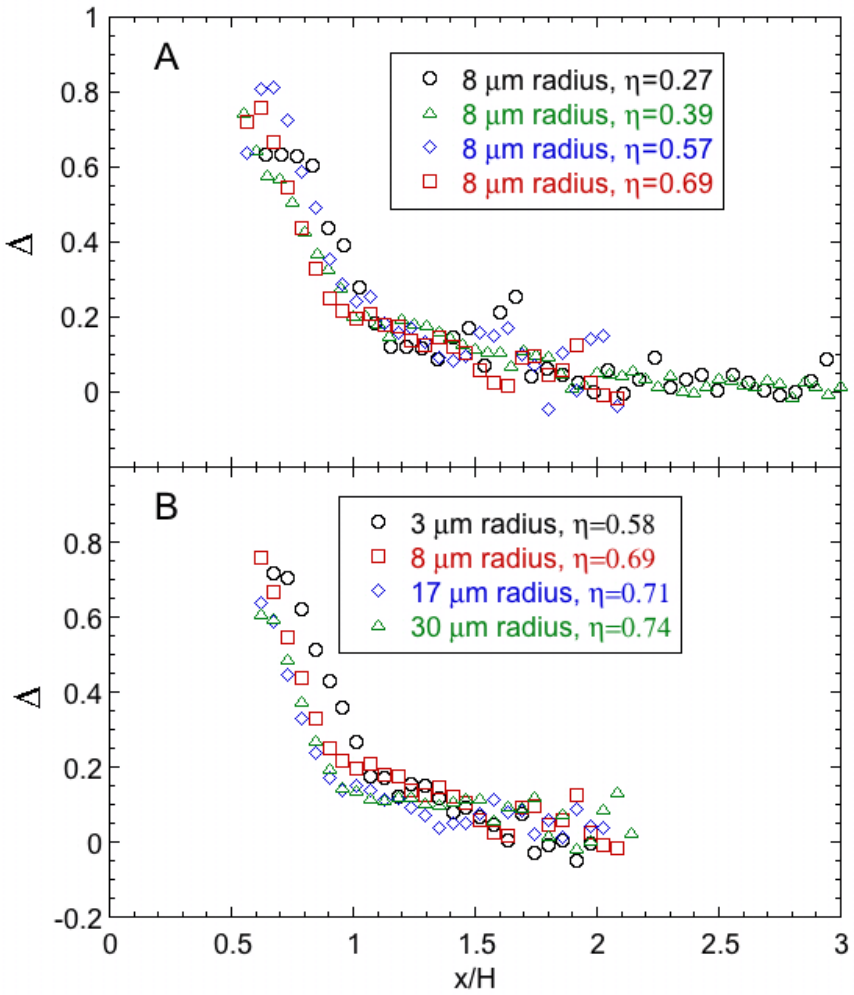

Figure 6: Color online. Normalized pair diffusion coefficients for various circular channels. There is no apparent dependence of the pair diffusion on either the curvature of the ring, or the density of the system (except possibly in the limiting case of a 3 μm ring, in which the approximation of a q1D system begins to break down). This implies that, as expected, correlations in the high q regime are locally determined.

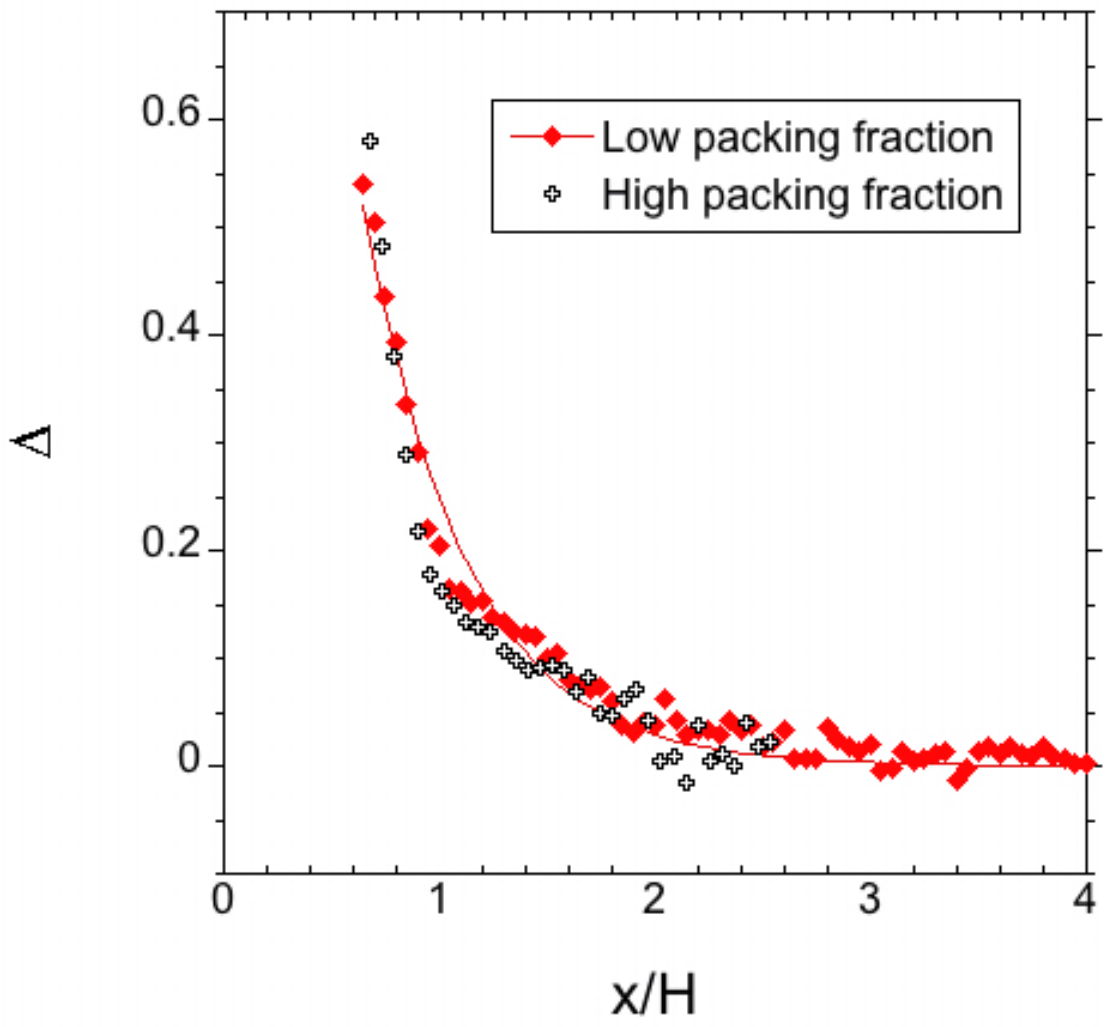

Figure 7: Color online. Normalized pair-diffusion coefficients Δ for the circular channels at lower and higher packing fractions, respectively, as a function of distance x scaled by channel width H. The solid line represents the fit of the lower packing fraction data to Eq. (13).

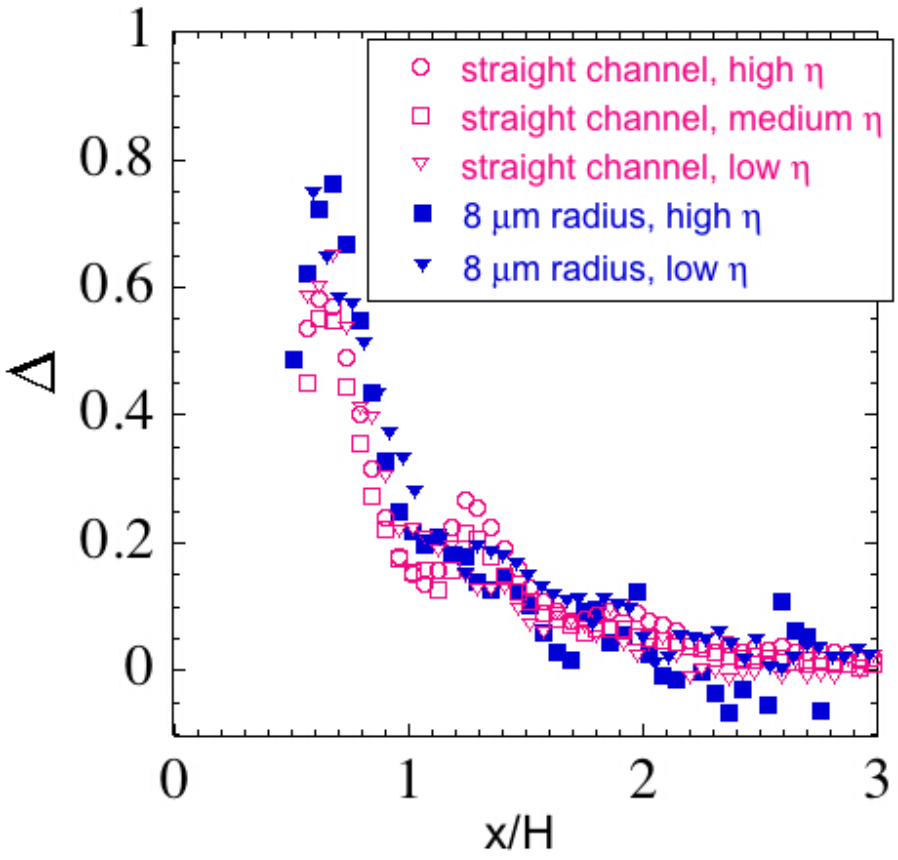

Figure 8: Color online. Normalized pair diffusion coefficients Δ for straight channels and rings, as a function of distance *x* scaled by channel width *H*. Note that there does not appear to be an observable difference in measured pair diffusion between the two data sets.